

## Electronic Supplementary Information

### *New Journal of Chemistry*

#### **Water-soluble naphthalimide-based ‘Pourbaix Sensors’: pH and redox-activated fluorescent AND logic gates based on photoinduced electron transfer**

Alex D. Johnson,<sup>a</sup> Kyle A. Paterson,<sup>a</sup> Jake C. Spiteri,<sup>a</sup> Sergey A. Denisov,<sup>b</sup> Gediminas Jonusauskas,<sup>c</sup> Arnaud Tron,<sup>b</sup> Nathan D. McClenaghan<sup>b</sup> and David C. Magri\*<sup>a</sup>

<sup>a</sup>*Department of Chemistry, Faculty of Science, University of Malta, Msida, MSD 2080, Malta. E-mail: david.magri@um.edu.mt*

<sup>b</sup>*Institut des Sciences Moléculaires, CNRS UMR 5255, University Bordeaux, 33405 Talence, France. E-mail: nathan.mcclenaghan@u-bordeaux.fr*

<sup>c</sup>*Laboratoire Ondes et Matières d'Aquitaine, CNRS UMR 5798, University of Bordeaux, 33405 Talence, France.*

## Table of Contents

<b>Fig. S1.</b> $^1\text{H}$ NMR spectrum of <b>1</b> in $\text{CDCl}_3$ .....	3
<b>Fig. S2.</b> $^{13}\text{C}$ NMR Spectrum of <b>2</b> in $\text{CDCl}_3$ .....	4
<b>Fig. S3.</b> Infra-red spectrum of <b>1</b> as a thin film on a NaCl disc.....	5
<b>Fig. S4.</b> $^1\text{H}$ NMR spectrum of compound <b>2</b> in $\text{CDCl}_3$ .....	6
<b>Fig. S5.</b> $^{13}\text{C}$ NMR spectrum of compound <b>2</b> in $\text{CDCl}_3$ .....	7
<b>Fig. S6.</b> IR spectrum of <b>2</b> collected using a solvent cell with $\text{CHCl}_3$ .....	8
<b>Fig. S7.</b> UV-visible absorption spectra of $5\ \mu\text{M}$ <b>1</b> in 1:1 (v/v) MeOH/ $\text{H}_2\text{O}$ from pH 11.7 to pH 2.7.....	9
<b>Fig. S8.</b> UV-visible absorption spectra of $5\ \mu\text{M}$ <b>1</b> in 1:1 (v/v) MeOH/ $\text{H}_2\text{O}$ on addition of up to 40 equivalence of $\text{Fe}^{3+}$ ( $200\ \mu\text{M}$ ).....	9
<b>Fig. S9.</b> UV-visible absorption spectra of $3\ \mu\text{M}$ <b>2</b> as a function of pH in presence of $80\ \mu\text{M}$ $\text{Fe}^{3+}$ in 1:1 (v/v) MeOH/ $\text{H}_2\text{O}$ .....	10
<b>Fig. S10.</b> UV-visible absorption spectra of $3\ \mu\text{M}$ <b>2</b> at pH 5 on addition of $\text{Fe}^{3+}$ in 1:1 (v/v) MeOH/ $\text{H}_2\text{O}$ .....	10
<b>Fig. S11.</b> Solutions of $10^{-5}\ \text{M}$ <b>2</b> in methanol in the presence of (A) no inputs, (B) $10^{-6.0}\ \text{M}$ $\text{CH}_3\text{SO}_3\text{H}$ , (C) $70\ \mu\text{M}$ $\text{Fe}^{3+}$ , (D) $70\ \mu\text{M}$ $\text{Fe}^{3+}$ and $10^{-6.0}\ \text{M}$ $\text{CH}_3\text{SO}_3\text{H}$ under UV illumination at 365 nm.....	11
<b>Fig. S12.</b> Fluorescence emission spectra of $4\ \mu\text{M}$ <b>1</b> as a function of pH in 1:1 (v/v) MeOH/ $\text{H}_2\text{O}$ excited at 438 nm.....	12
<b>Fig. S13.</b> Fluorescence titration plot of $4\ \mu\text{M}$ <b>1</b> as a function of pH in 1:1 (v/v) MeOH/ $\text{H}_2\text{O}$ . Inset: Linearised Henderson-Hasselbalch plot based on the fluorescence intensity at 526 nm. ....	12
<b>Fig. S14.</b> Fluorescence emission spectra of $3\ \mu\text{M}$ <b>2</b> as a function of pH in the presence of $80\ \mu\text{M}$ $\text{Fe}^{3+}$ in 1:1 (v/v) MeOH/ $\text{H}_2\text{O}$ excited at 437 nm.....	13
<b>Fig. S15.</b> Fluorescence titration plot of $3\ \mu\text{M}$ <b>2</b> as a function of pH in the presence of $80\ \mu\text{M}$ $\text{Fe}^{3+}$ in 1:1 (v/v) MeOH/ $\text{H}_2\text{O}$ . Inset: Linearised Henderson-Hasselbalch plot based on the fluorescence intensity at 535 nm. ....	13
<b>Fig. S16.</b> Fluorescence emission spectra of $3\ \mu\text{M}$ <b>2</b> in the presence of $80\ \mu\text{M}$ $\text{Fe}^{3+}$ as a function of $\text{p}\beta_{\text{H}^+}$ in methanol excited at 432 nm.....	14
<b>Fig. S17.</b> Fluorescence titration of $3\ \mu\text{M}$ <b>2</b> in the presence of $80\ \mu\text{M}$ $\text{Fe}^{3+}$ as a function of $\text{p}\beta_{\text{H}^+}$ in methanol. Inset: Linearised Henderson-Hasselbalch plot based on the fluorescence intensity at 530 nm. ....	14
<b>Fig. S18.</b> Scheme for sub-nanosecond laser set-up; SHG/THG – second/third harmonic generator, OPG – optical parametric generator, LED – light emitting diode, DSG – digital signal generator.....	15
<b>Fig. S19.</b> Scheme of sub-picosecond laser set-up; OPG – optical parametric generator; BBO – barium borate crystal.....	16
<b>Fig. S20.</b> Luminescence decay of <b>3</b> at pH 4 in 1:1 (v/v) MeOH/ $\text{H}_2\text{O}$ in the presence of $\text{Fe}^{3+}$ .....	17
Steady-state absorption and photoluminescence measurements.....	17

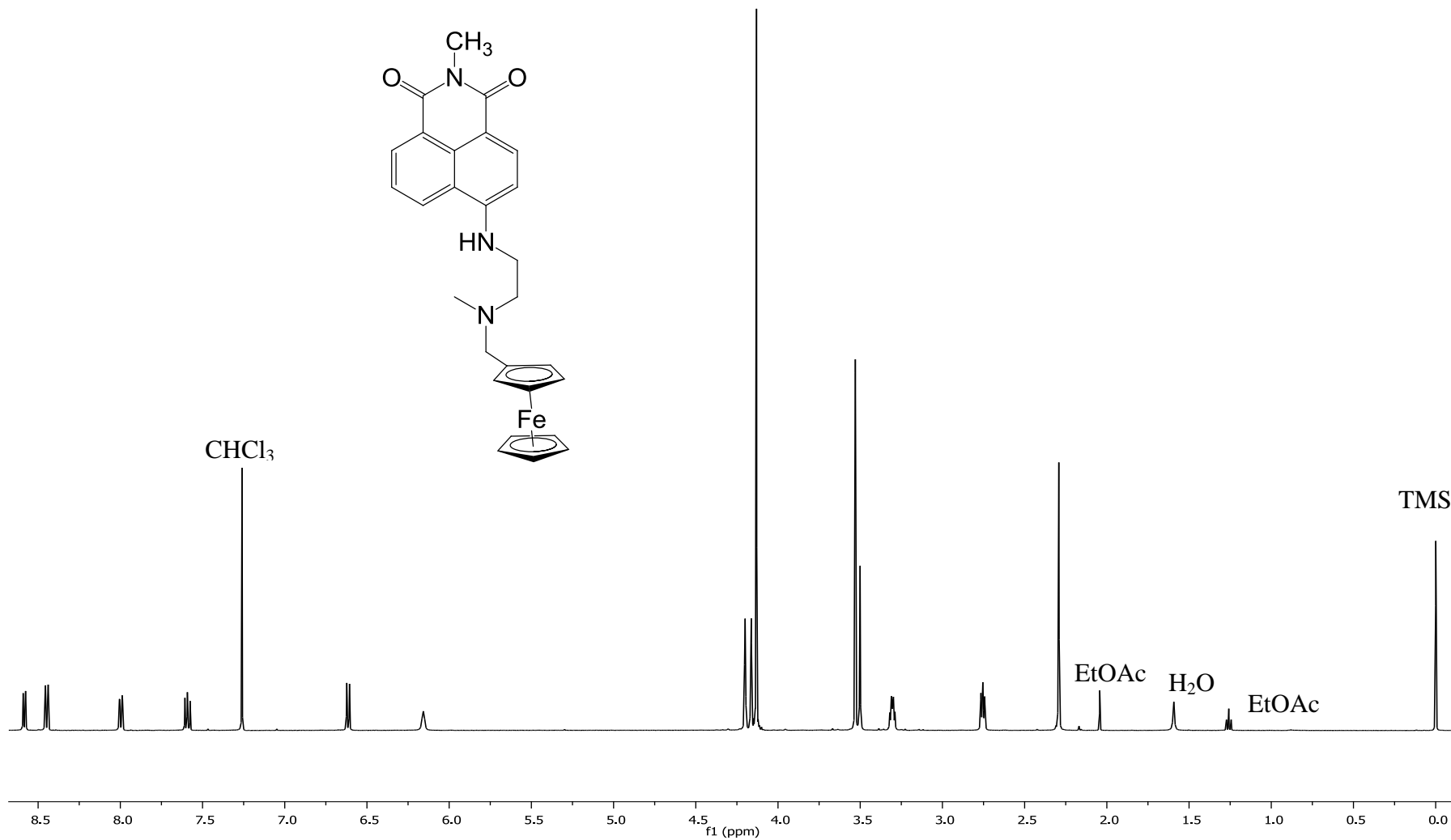


**Fig. S1.** <sup>1</sup>H NMR spectrum of **1** in CDCl<sub>3</sub>.

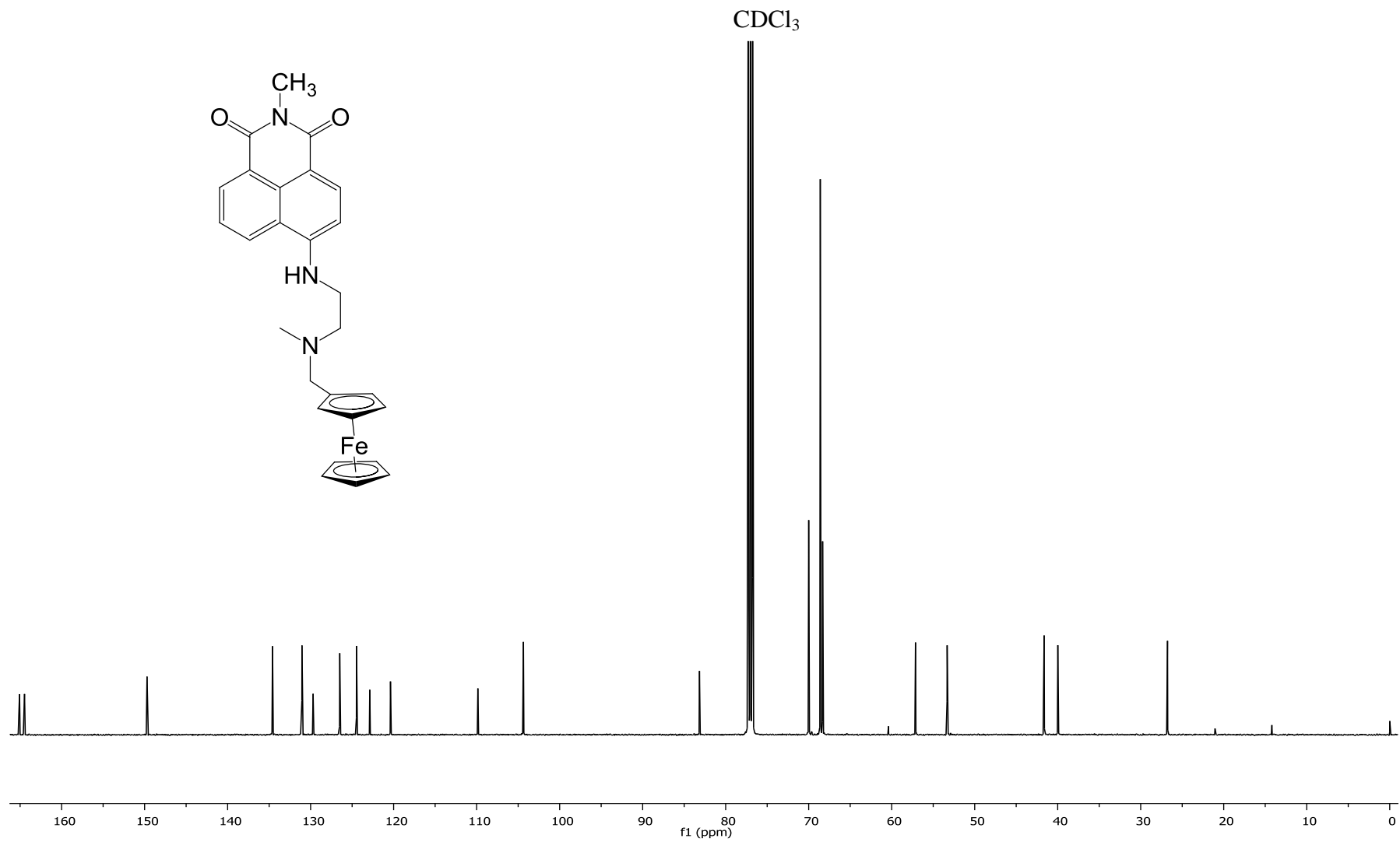


**Fig. S2.**  $^{13}\text{C}$  NMR Spectrum of **2** in  $\text{CDCl}_3$ .

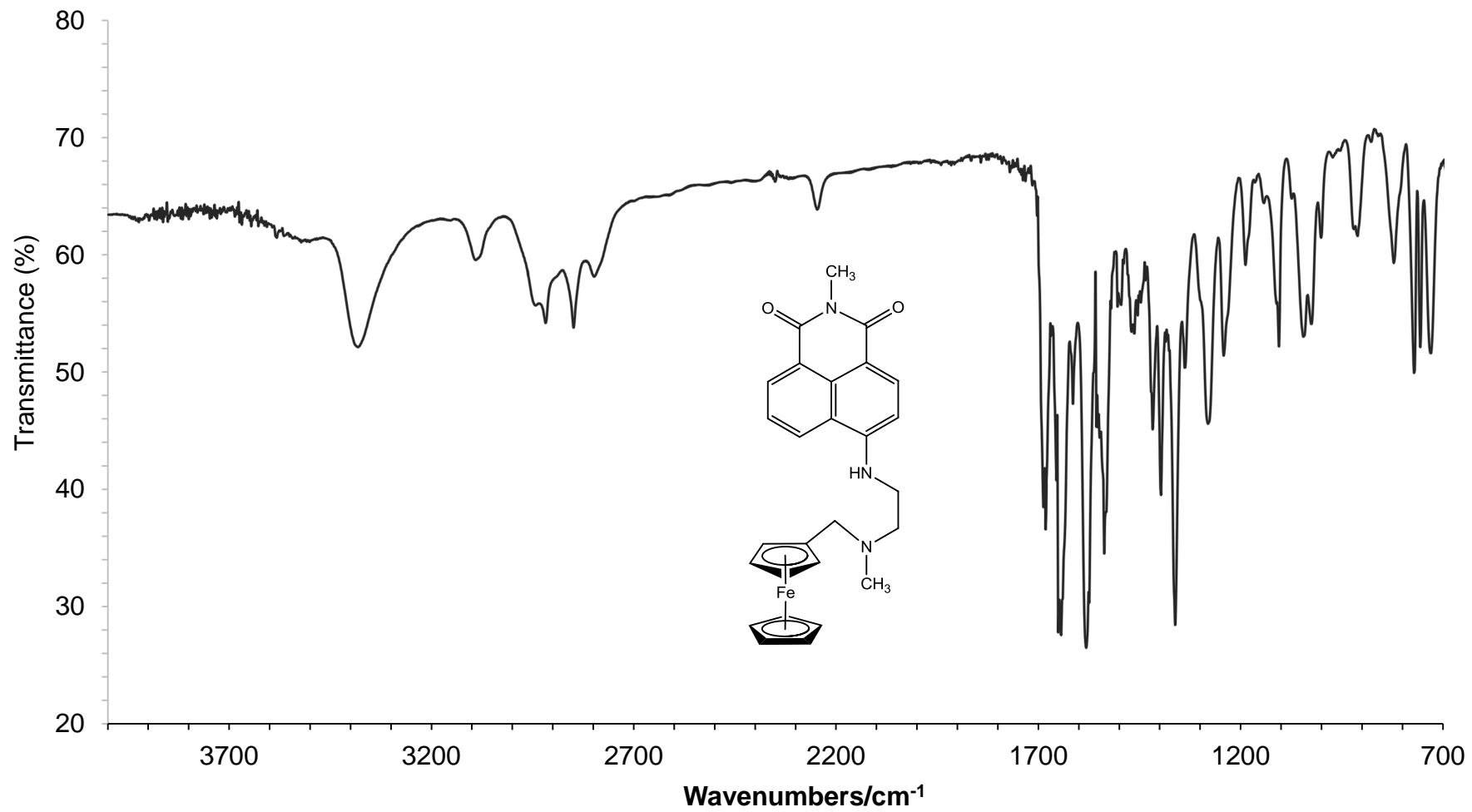


**Fig. S3.** Infra-red spectrum of **1** as a thin film on a NaCl disc.

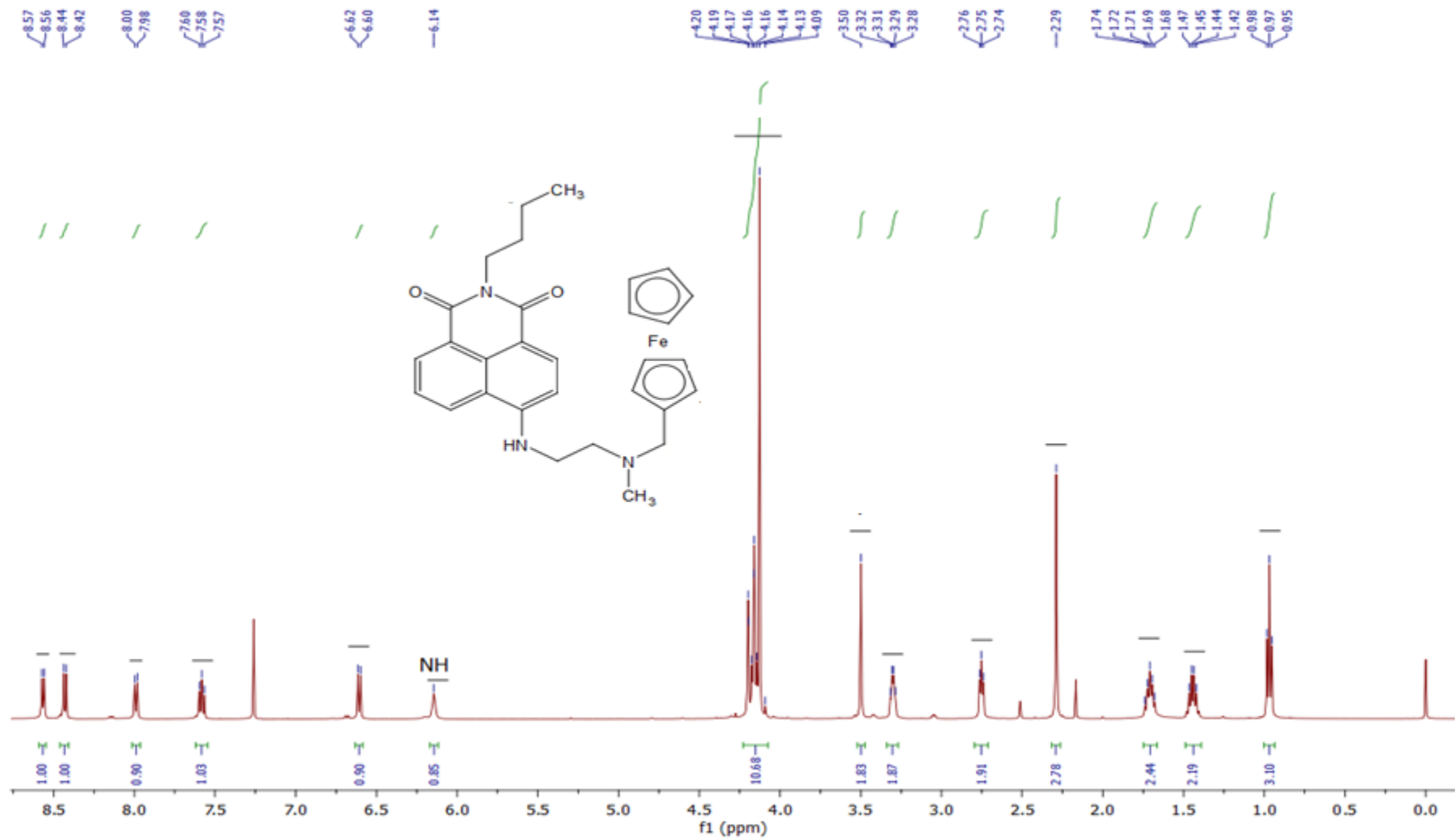
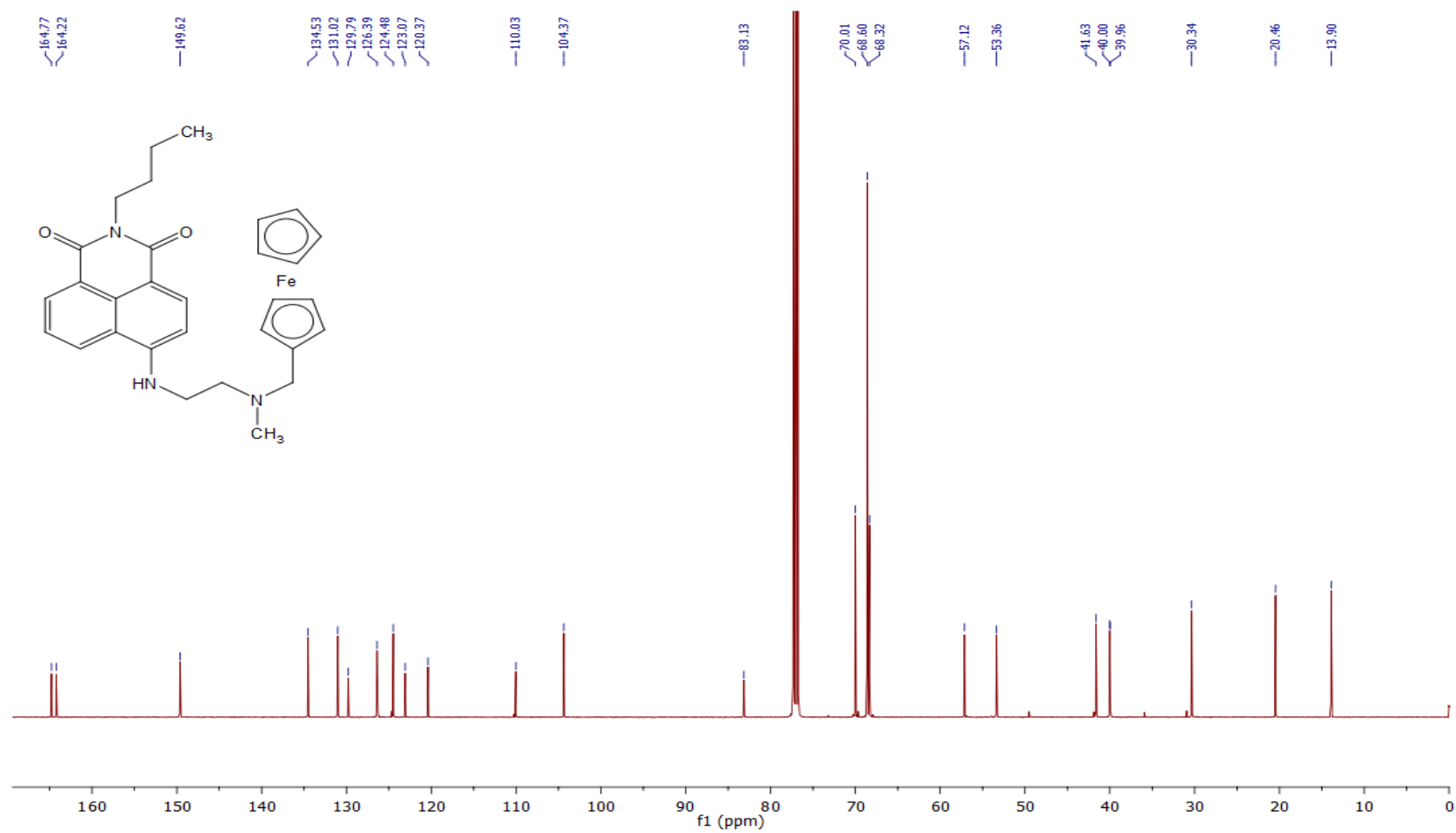
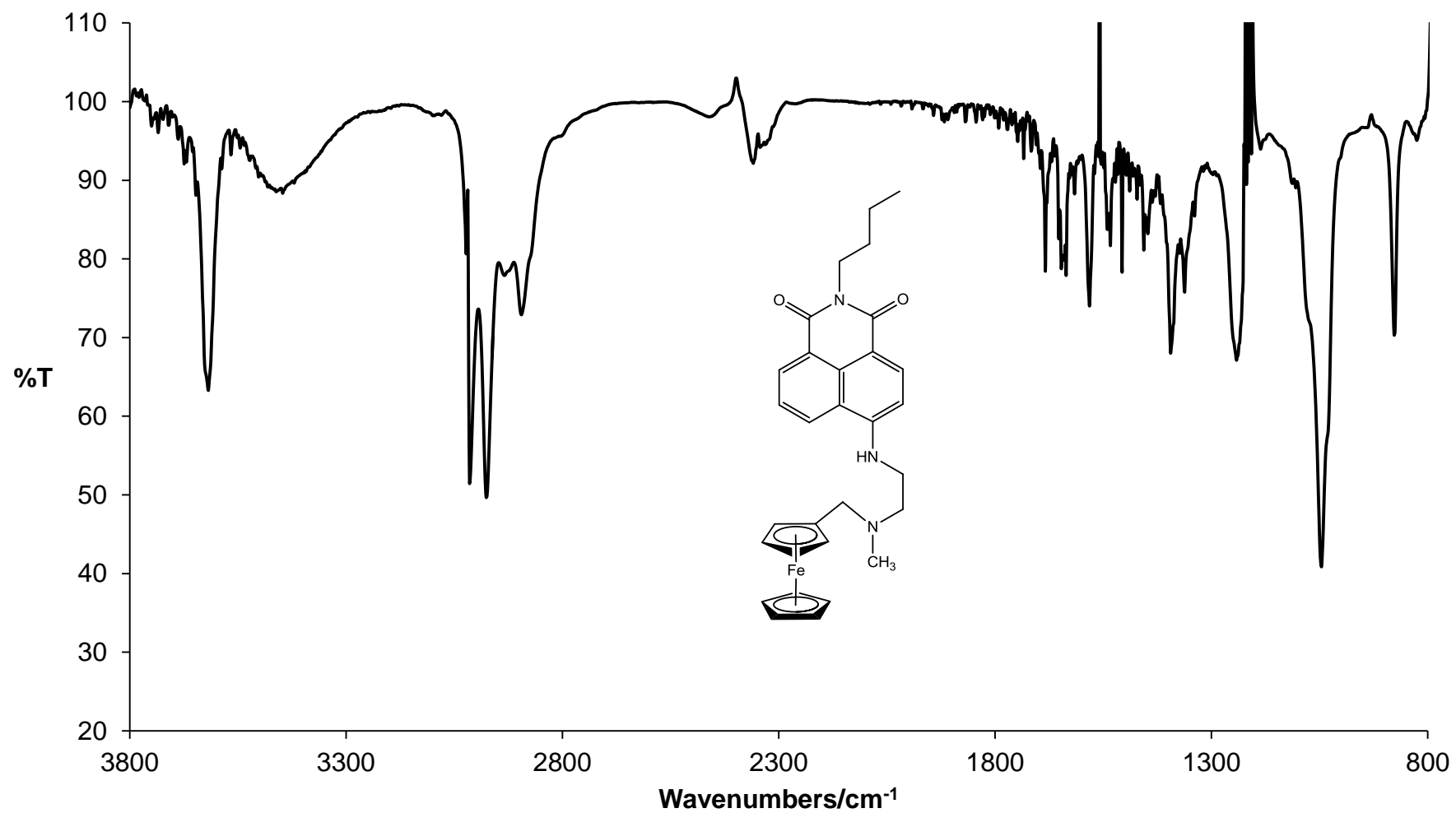


Fig. S4. <sup>1</sup>H NMR spectrum of compound 2 in CDCl<sub>3</sub>.



**Fig. S5.** <sup>13</sup>C NMR spectrum of compound **2** in CDCl<sub>3</sub>.



**Fig. S6.** IR spectrum of **2** collected in a solvent cell with CHCl<sub>3</sub>.

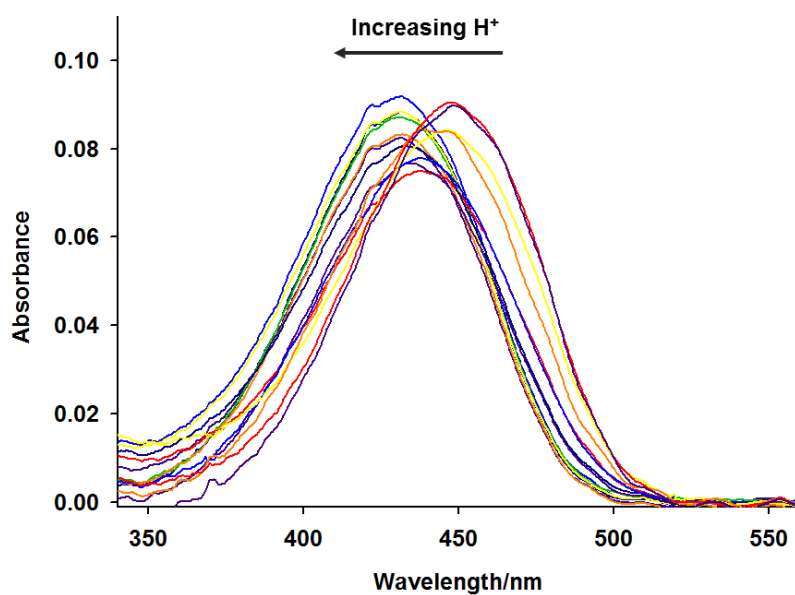


**Fig. S7.** UV-visible absorption spectra of 5 μM **1** in 1:1 (v/v) MeOH/H<sub>2</sub>O from pH 11.7 to pH 2.7.

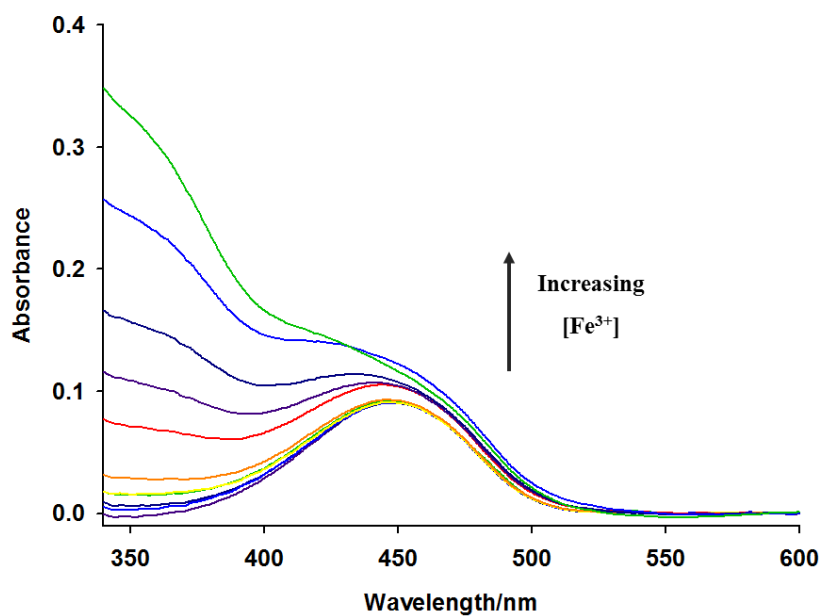


**Fig. S8.** UV-visible absorption spectra of 5 μM **1** in 1:1 (v/v) MeOH/H<sub>2</sub>O on addition of up to 40 equivalence of Fe<sup>3+</sup> (200 μM).

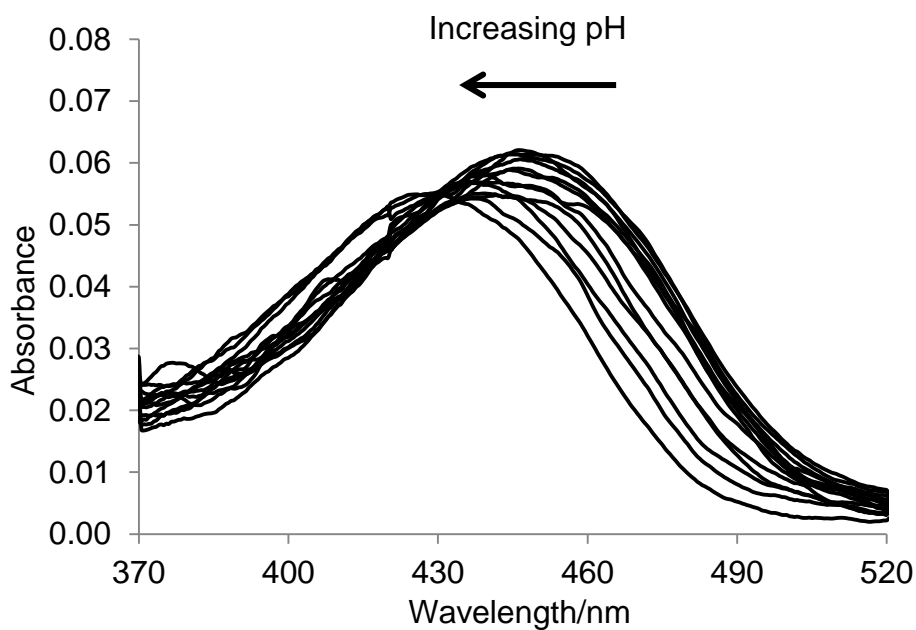


**Fig. S9.** UV-visible absorption spectra 3 μM **2** as a function of pH in presence of 80 μM Fe<sup>3+</sup> in 1:1 (v/v) MeOH/H<sub>2</sub>O.

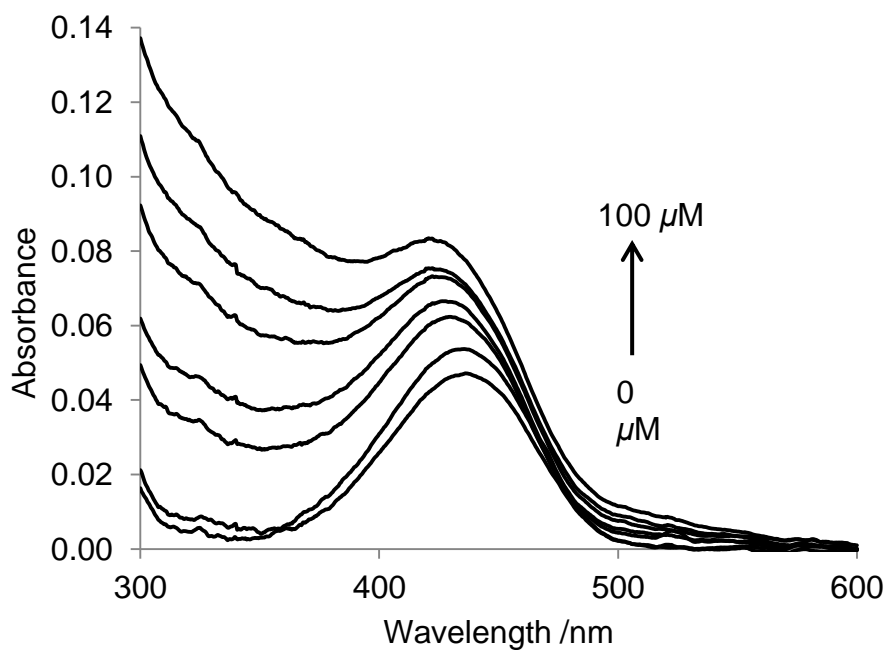


**Fig. S10.** UV-visible absorption spectra of 3 μM **2** at pH 5 on addition of Fe<sup>3+</sup> in 1:1 (v/v) MeOH/H<sub>2</sub>O.

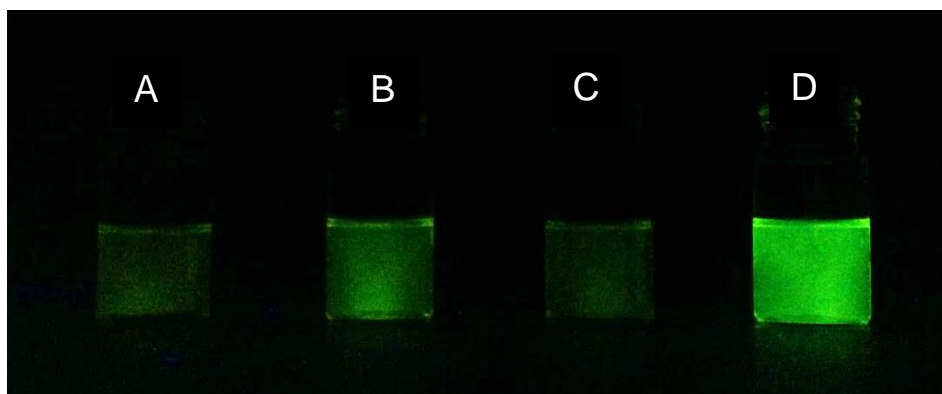


**Fig. S11.** Solutions of  $10^{-5}$  M **2** in methanol in the presence of (A) no inputs, (B)  $10^{-6.0}$  M  $\text{CH}_3\text{SO}_3\text{H}$ , (C)  $70 \mu\text{M Fe}^{3+}$ , (D)  $70 \mu\text{M Fe}^{3+}$  and  $10^{-6.0}$  M  $\text{CH}_3\text{SO}_3\text{H}$  under UV illumination at 365 nm.

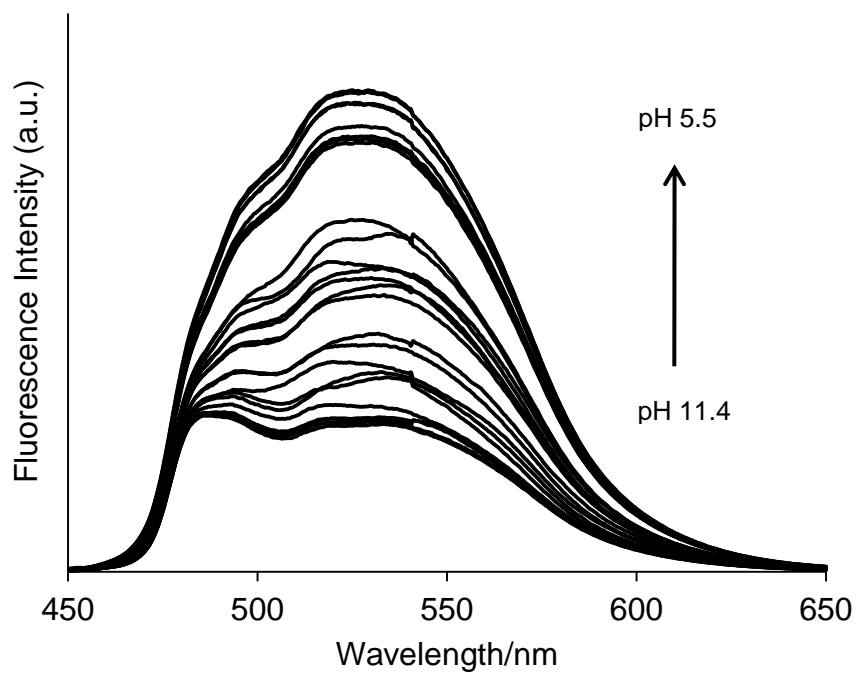


**Fig. S12.** Fluorescence emission spectra of 4  $\mu\text{M}$  **1** as a function of pH in 1:1 (v/v) MeOH/H<sub>2</sub>O excited at 438 nm.

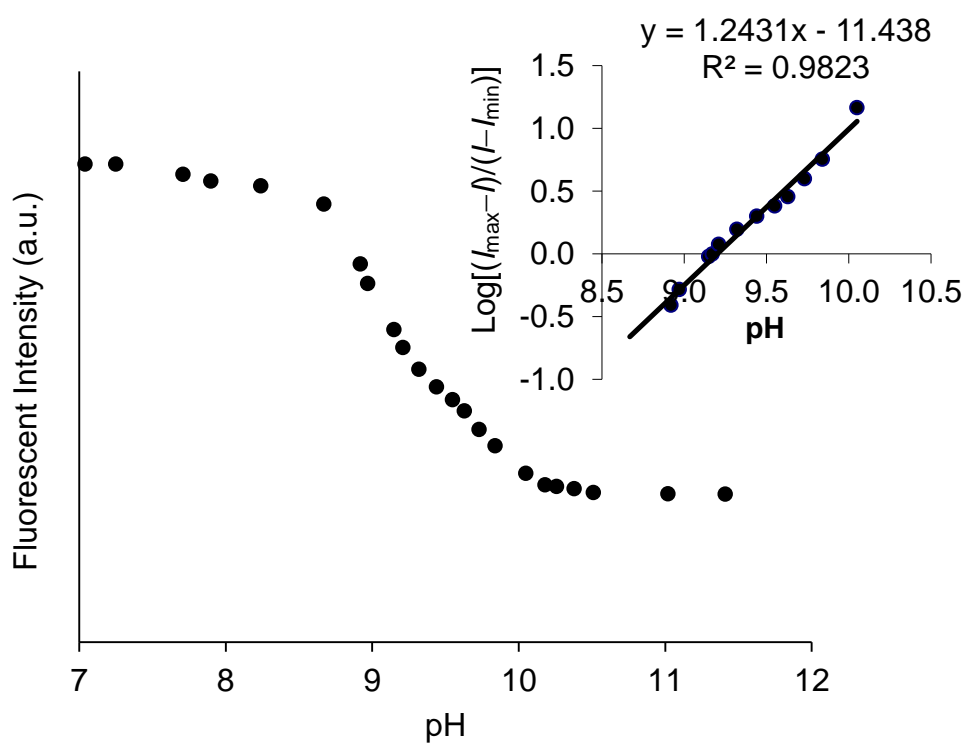


**Fig. S13.** Fluorescence titration plot of 4  $\mu\text{M}$  **1** as a function of pH in 1:1 (v/v) MeOH/H<sub>2</sub>O. Inset: Linearised Henderson-Hasselbalch plot based on the fluorescence intensity at 526 nm.

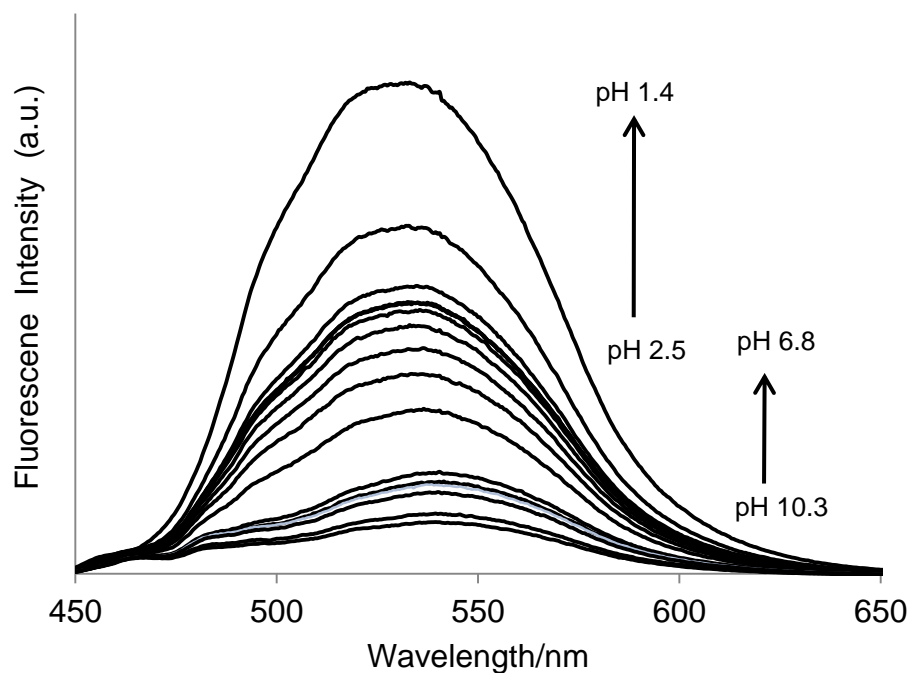


**Fig. S14.** Fluorescence emission spectra of 3  $\mu\text{M}$  **2** as a function of pH in the presence of 80  $\mu\text{M}$   $\text{Fe}^{3+}$  in 1:1 (v/v) MeOH/H<sub>2</sub>O excited at 437 nm.

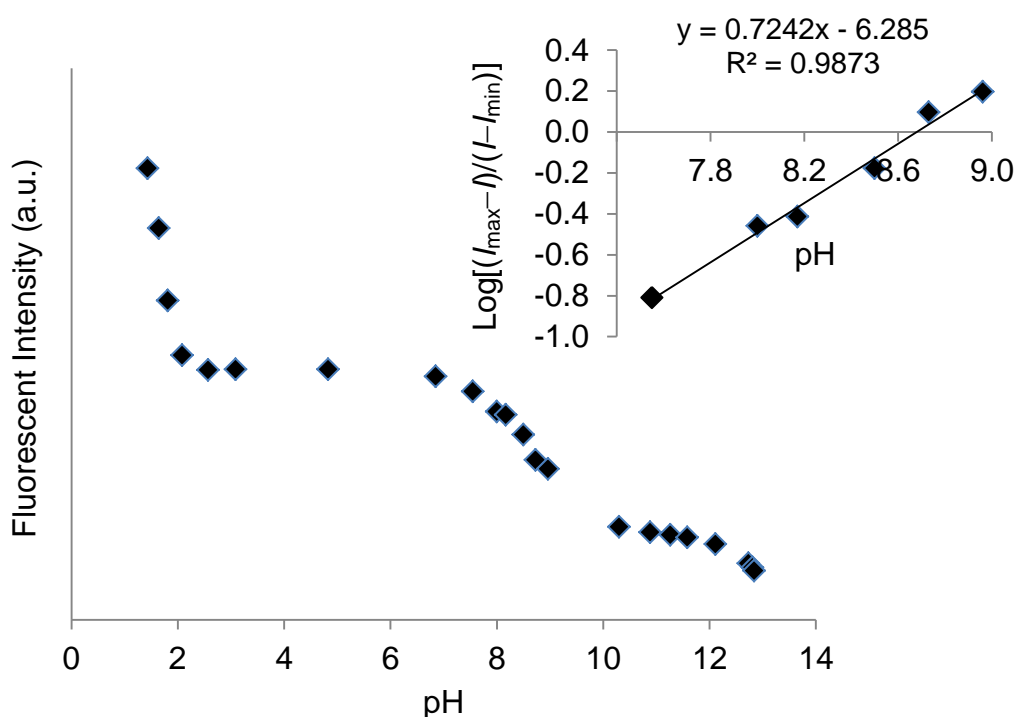


**Fig. S15.** Fluorescence titration plot of 3  $\mu\text{M}$  **2** as a function of pH in the presence of 80  $\mu\text{M}$   $\text{Fe}^{3+}$  in 1:1 (v/v) MeOH/H<sub>2</sub>O. Inset: Linearised Henderson-Hasselbalch plot based on the fluorescence intensity at 535 nm.

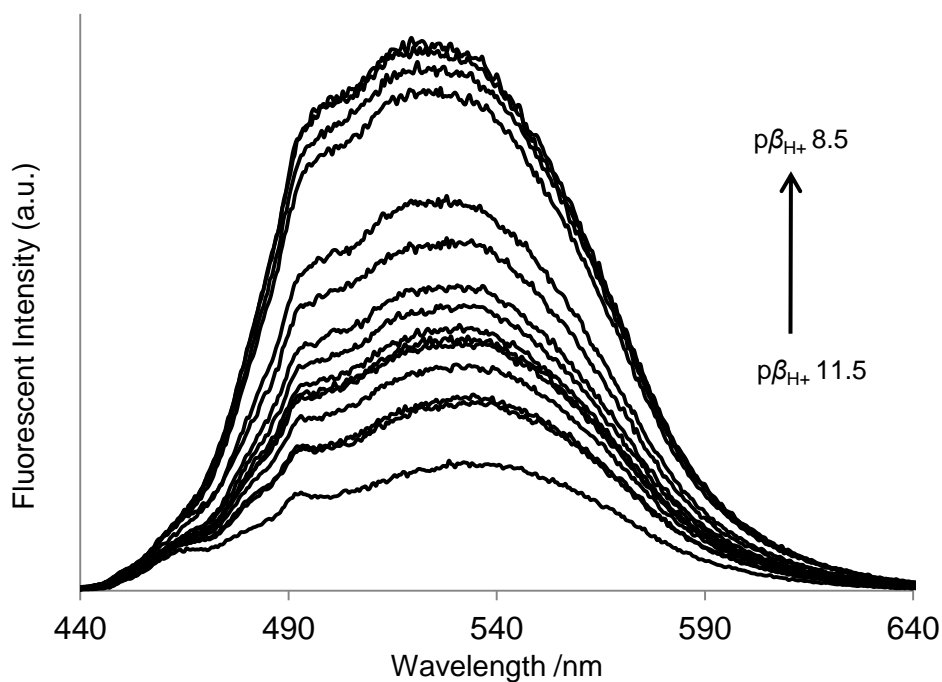


**Fig.S16.** Fluorescence emission spectra of 3  $\mu\text{M}$  **2** in the presence of 80  $\mu\text{M}$   $\text{Fe}^{3+}$  as a function of  $\text{p}\beta_{\text{H}^+}$  in methanol excited at 432 nm.

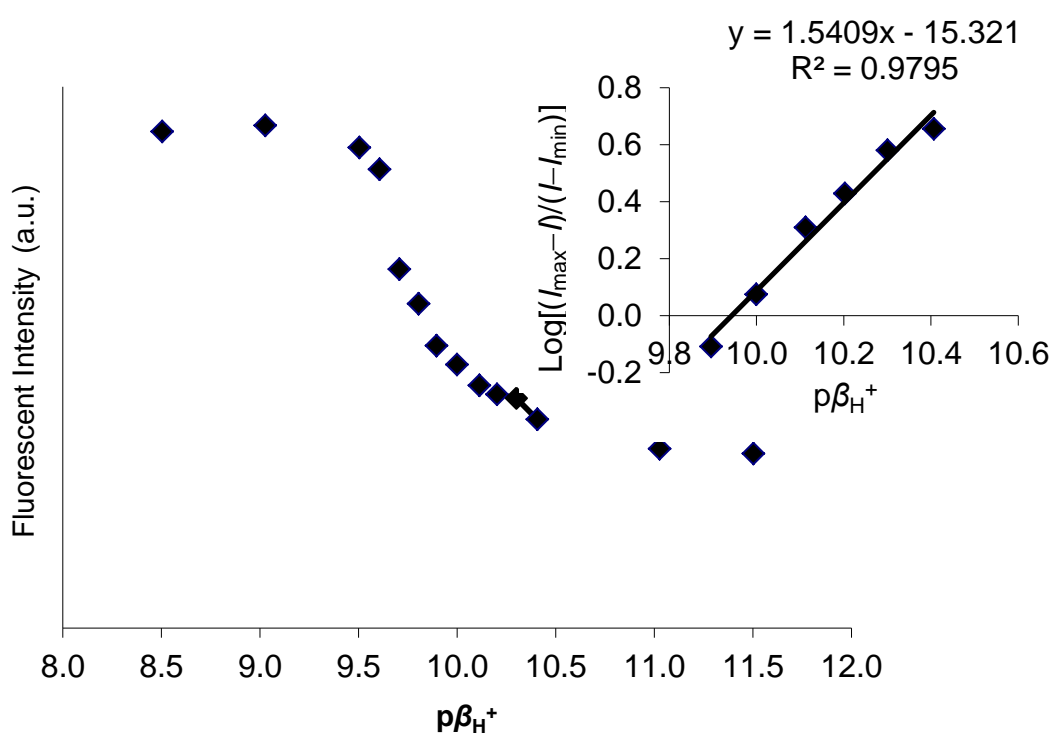


**Fig. S17.** Fluorescence titration of 3  $\mu\text{M}$  **2** in the presence of 80  $\mu\text{M}$   $\text{Fe}^{3+}$  as a function of  $\text{p}\beta_{\text{H}^+}$  in methanol. Inset: Linearised Henderson-Hasselbalch plot based on the fluorescence intensity at 530 nm.

## Time-resolved measurements

The time-resolved luminescence set-up was built as follows (Fig. S18): a frequency tripled Nd:YAG amplified laser system (30 ps, 30 mJ @1064 nm, 20 Hz, Ekspla model PL 2143) output was used to pump an optical parametric generator (Ekspla model PG 401) producing tunable excitation pulses in the range 410–2300 nm. The residual fundamental laser radiation was focused in a high pressure Xe filled breakdown cell where a white light pulse for sample probing was produced. For longer scales (micro- and milliseconds), the white light probe was obtained using an ensemble of light emitting diodes (Roithner Lasertechnik, from 365 to 710 nm) working in flash mode in a multi-furcated fiberoptic cable (8-cores, Avantes). All light signals were analysed by a spectrograph (Princeton Instruments Acton model SP2300) coupled with a high dynamic range streak camera (Hamamatsu C7700, 1ns-1ms). Accumulated sequences (sample emission, probe without and with excitation) of pulses were recorded and treated by HPDTA (Hamamatsu) software to produce two-dimensional maps (wavelength vs delay) of transient absorption intensity in the range 300–800 nm. Typical measurement error was better than  $10^{-3}$  O. D. Data were analysed using home-made software developed in LabVIEW 2014 system-design platform and development environment. The trust-region dogleg algorithm (supported by LabVIEW 2014) was applied to determine the set of parameters that best fit the set of input data. The trust-region dogleg algorithm was used instead of Levenberg-Marquardt algorithm, the latter being less stable in most cases during optimization process, because trust region methods are robust, and can be applied to ill-conditioned problems.

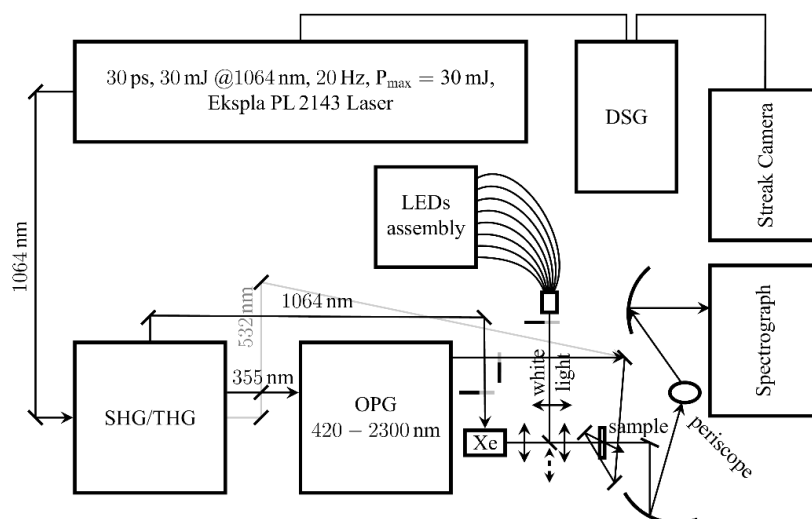


**Fig. S18.** Scheme for sub-nanosecond laser set-up; SHG/THG – second/third harmonic generator, OPG – optical parametric generator, LED – light emitting diode, DSG – digital signal generator.

The subpicosecond time scale set-up was based on a femtosecond 1 kHz Ti:sapphire system (Fig. S19) producing 30 fs, 0.8 mJ, laser pulses centred at 800 nm (Femtopower Compact Pro) coupled with an optical parametric generator (Light Conversion Topas C) and frequency mixers to excite samples at the maximum of the steady-state absorption band. White-light continuum (360–1000 nm) pulses generated in a 2 mm D<sub>2</sub>O cell were used as a probe. A variable delay time between excitation and probe pulses was obtained using a delay line with 0.66 fs resolution. The solutions were placed in a 1 mm circulating cell. Whitelight signal and reference spectra were recorded using a two-channel fibre spectrometer (Avantes Avaspec-2048-2). A home written acquisition and experiment control program in LabVIEW enabled the recording of transient spectra with an average error of less than  $10^{-3}$  of the optical density for all wavelengths. The temporal resolution of the setup was better than 50 fs. A temporal chirp of the probe pulse was corrected by a computer program with respect to a Lawrencian fit of a Kerr signal generated in a 0.2 mm glass plate used in place of a sample.

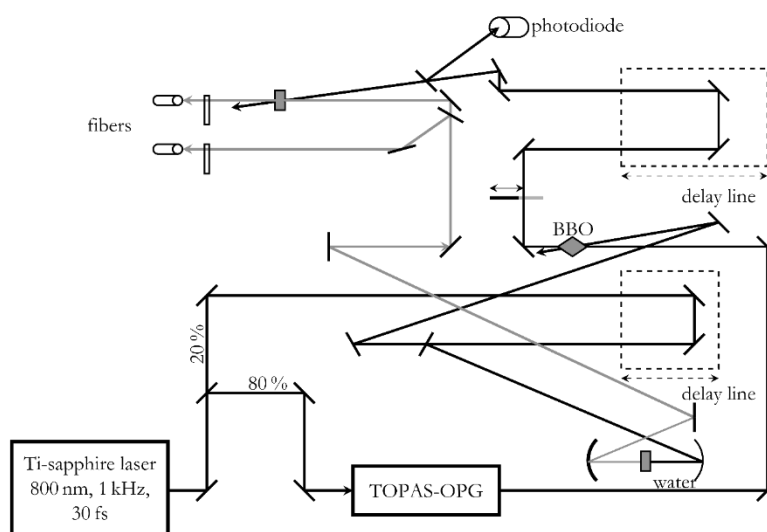


**Fig. S19.** Scheme of sub-picosecond laser set-up; OPG – optical parametric generator; BBO – barium borate crystal.

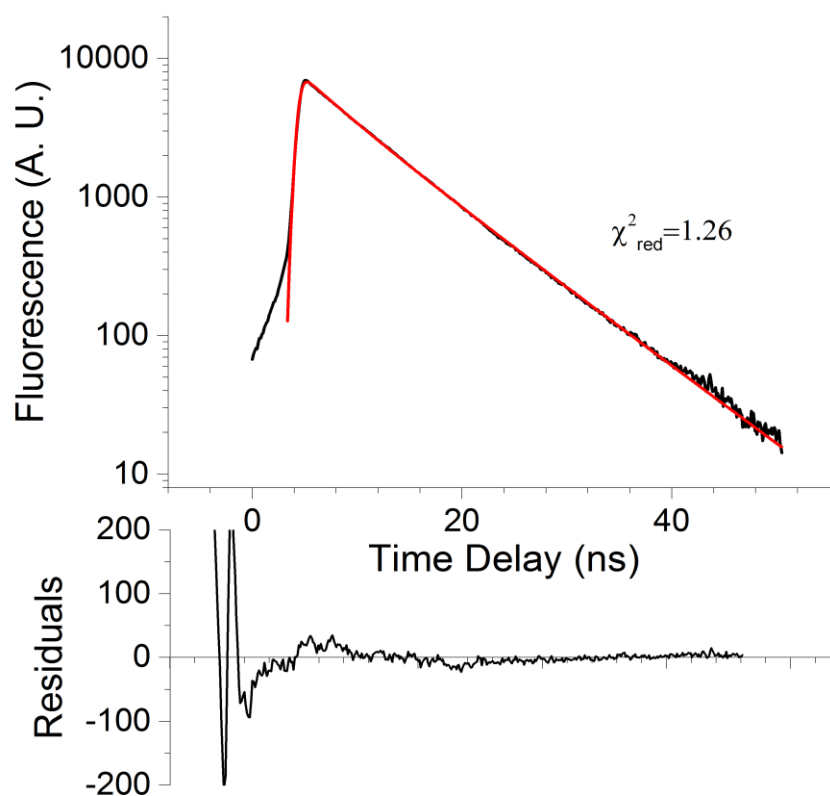


**Fig. S20.** Luminescence decay of **3** at pH 4 in 1:1(v/v) MeOH:H<sub>2</sub>O in presence of Fe<sup>3+</sup>.

### Steady-state absorption and photoluminescence measurements

UV-visible absorption spectra were recorded on a Jasco V-650 spectrophotometer using quartz Suprasil cells with a 10 mm pathlength. The instrumentation parameters were set to medium response, a bandwidth of 2 nm and a scan speed of 200 nm min<sup>-1</sup>. Samples were scanned between 350-600 nm. All spectra were corrected for the solvent by scanning the appropriate blank solvent prior to beginning the experiments setting the baseline.

Fluorimetric studies were conducted using a Jasco FP-8300 spectrophotometer with 10 mm path length quartz cuvette. The excitation wavelength was set at the isosbestic point. Bandwidths of 2.5 nm and 5.0 nm were used for the excitation and emission slits with a scan speed of 200 nm min<sup>-1</sup>. The emission range was 420-670 nm, unless otherwise stated. Fluorescence quantum yield studies of degassed solutions were performed using a Fluorolog-3 (Jobin Yvon) spectrofluorometer with iHR-320 and photomultipliers from Hamamatsu Photonics: R2658 (range 280–1100 nm) with reference to 10<sup>-7</sup> M fluorescein in 0.1 M NaOH aerated water ( $\Phi_F = 0.91$ ).